International Journal of Industrial Chemistry (2018) 9:105–114
https://doi.org/10.1007/s40090-018-0142-7

RESEARCH

Efficacies of sodium nitrite and sodium citrate–zinc acetate mixture to inhibit steel rebar corrosion in simulated concrete interstitial solution contaminated with NaCl

Binsi Paulson Maliekkal[1] · Joby Thomas Kakkassery[1] · Vinod Raphael Palayoor[2]

Received: 6 September 2017 / Accepted: 20 March 2018 / Published online: 4 April 2018

Abstract
Investigations were carried out to compare the effectiveness of compounds such as sodium nitrite, trisodium citrate (TSC) and TSC–zinc acetate to inhibit the corrosion of steel rebar in simulated concrete interstitial solution contaminated with chloride and to explain the mechanism of corrosion inhibition on reinforcing steel by these systems. Inhibition efficiency of these systems was studied by electrochemical techniques such as potentiodynamic polarization and half cell potential measurements. Electronic spectral studies of simulated pore solution and FT-IR spectral investigations of the film deposited on steel surface were carried out for understanding the mechanism of corrosion inhibition. Microscopic surface analysis was conducted to obtain the surface morphological behaviour of steel rebar. TSC alone was not exhibited good corrosion inhibition at very low and high concentrations according to electrochemical studies. However, in the presence of zinc acetate, corrosion protection efficiency of TSC increased appreciably. When comparing with sodium nitrite, TSC in the presence and absence of zinc acetate displayed good corrosion inhibition efficiency. Among a number of samples, TSC 100 ppm-zinc acetate 50 ppm combination showed maximum corrosion inhibition efficiency on steel rebar in simulated concrete interstitial solution.

Keywords Corrosion · Inhibitor · Trisodium citrate · Reinforced concrete

Introduction

Premature deterioration of concrete structures mainly occurs due to the ingress of chloride ions and carbon dioxide [1]. Chloride ions make local depassivation of the steel rebar leading to pitting corrosion [2–5]. Carbon dioxide reacts with the alkaline compounds present in concrete leading to lower pH and consequent loss of passivation of the rebars [6–9]. Among a few procedures available to minimize the corrosion of steel rebar in concrete, the use of corrosion inhibitors has been envisaged as the most practical solution [10–14]. An ideal corrosion inhibitor is a chemical substance which when added to concrete, prevent corrosion onset without making any adverse effects on the mechanical properties of the concrete. It has been generally accepted that inhibitors influence the kinetics of the electrochemical reactions involved in the corrosion process occurring in steel [15–17].

The mechanisms by which corrosion inhibitors are able to protect reinforcing steel have been discussed in the literature and include (1) decrease in the diffusion rate of the chloride ion (2) increase in the amount of bound chloride (3) increase in the chloride ion threshold value or (4) inhibition of the anodic, cathodic or both reactions [18–21]. There are some controversies existing about the inhibition mechanism and protection efficiency of corrosion inhibitors. Some authors argue that those compounds which are used to protect concrete reinforcement are not effective [10] when the concrete is kept immersed in NaCl solution, whereas others report that some compounds are effective in reducing corrosion rate of steel rebar in concrete contaminated with chlorides [22, 23].

The inhibitors commonly used to control the reinforcement corrosion are usually classified in two: (1) inhibitors that can

Electronic supplementary material The online version of this article (https://doi.org/10.1007/s40090-018-0142-7) contains supplementary material, which is available to authorized users.

✉ Joby Thomas Kakkassery
drjobythomask@gmail.com

[1] Research Division, Department of Chemistry, St. Thomas' College (Autonomous), Thrissur, Kerala 680001, India

[2] Department of Chemistry, Government Engineering College, Thrissur, Kerala 680009, India

be mixed with fresh concrete mixture and applied in reinforced structures (admixture) and (2) inhibitors which are applied on the concrete surface during the rehabilitation procedures since they can diffuse into the hardened concrete (migrating corrosion inhibitors—MCI) [24–26]. Nowadays, some admixtures are available in the market, which are based on inorganic or organic compounds. Inorganic inhibitors are mainly consist of nitrites or sodium mono-fluoro-phosphate [27–29]. Effectiveness of nitrites as corrosion inhibitor has already been proved by various researchers [30–32]. Other organic corrosion inhibitors such as aminoethanols have also been studied; however, they are not as successful as nitrites [33–35]. Some organic water soluble admixtures are typically based on the mixtures of alkanolamines or organic acids. This kind of commercial inhibitors have been widely applied, but a very little is known about the mechanism of corrosion protection [36]. It is believed that these inhibitors are able to diffuse to the anodic or cathodic site (or both) on the steel surface and interfere the electrode reaction, and thus prevent corrosion initiation [37].

To investigate concrete rebar corrosion studies, researchers either depend upon actual concrete specimens or simulated concrete pore solution [38, 39]. Since first method is rather time consuming, many investigators adopt the second method as a quick procedure [40]. The choice of concrete pore solution gives an adequate support to study the corrosion behaviour of reinforcing steel in chemical conditions [33, 41].

In this work, corrosion inhibition efficacy of compounds such as trisodium citrate (TSC) and TSC–zinc acetate mixture on steel rebar in simulated concrete interstitial solution contaminated with NaCl was evaluated and compared with the corrosion inhibition efficacy of sodium nitrite on steel rebar in the same solution. The present investigation also aims to explain the behaviour of these chemical species on steel rebar in contaminated concrete pore solution.

Experimental

Materials

Chemicals such as trisodium citrate (98%), sodium chloride (> 99.9%), $NaNO_2$ (EMSURE®) and zinc acetate (> 99%) were purchased from Merck Millipore. Portland cement (Malabar Cements Ltd, Kerala) used for the preparation of aqueous extract was procured from the market.

Steel rebar having approximate composition 0.62% Mn, 0.1% P, 0.04% S, 0.021% Si, and rest Fe (estimated by EDAX technique—SEM, Hitachi SU6600 model) was cut (10 cm) and pickled with 2 M HCl for 20 min. Steel specimens were washed with distilled water, degreased with acetone and dried in hot air oven for 5 min. The working solution (concrete pore solution) was prepared by mixing cement with water having a water/cement ratio 0.5 [42]. Temperature of the cement–water mixture gradually increased due to exothermic nature of hydration of cement. The mixture was continuously stirred for 15–20 min using mechanical stirrer for maintaining the homogeneity and temperature stabilisation. The mixture was filtered using vacuum pump to obtain clear concrete pore solution (CPS). The pH of the solution was between 12.5 and 13. Approximate chemical composition of this solution was determined by volumetric and photometric methods and is given in Table 1. To 100 ml of concrete pore solution, 3.5 g of NaCl was added to achieve 3.5% NaCl concentration. To this, trisodium citrate (TSC) was added to attain the concentrations 50, 100, 150, 200 and 1500 ppm. Similarly, $NaNO_2$ solutions were prepared in CPS. Another set of sodium citrate solutions were also prepared (50–200 ppm) in CPS containing 50 ppm of zinc acetate (ZnAc).

Potentiodynamic polarization studies

Steel specimens were immersed in CPS for 3 days in the presence and absence of added compounds. Potentiodynamic polarization studies were carried out using three electrode cell assembly consisting of steel rod as working electrode (exposed area 4 cm^2), platinum electrode as counter electrode (1 cm^2) and saturated calomel electrode (SCE) as reference electrode at 30 °C. A potential range of + 250 to − 250 mV with a sweep rate of 1 mV/s was used for the study. Slope analysis of Tafel curves gave the corrosion current densities, and the inhibition efficiency was calculated by the following equation [43–45]:

$$\eta_{\text{pol}}\,\% = \frac{I_{\text{corr}} - I'_{\text{corr}}}{I_{\text{corr}}} \times 100,$$

where I_{corr} and I'_{corr} are the corrosion current densities of exposed area steel rebar in the absence and presence of inhibitor, respectively.

Half cell potential measurements

For a quick examination of the corrosion behaviour of steel rebar in various medium, half cell potential

Table 1 Composition of aqueous cement extract simulating the concrete interstitial electrolyte

Species	Ca^{2+}	SO_4^{2-}	Fe^{3+}	PO_4^{3-}	Cl^-	F^-	Mg^{2+}
Conc. (ppm)	854	6642	1700	7.54	214	4.89	< 2

measurements were carried out. After an equilibration period of 24 h, saturated calomel electrode (SCE) was immersed into solution containing steel rebar. The EMF of cell was measured using a high impedance voltmeter (HP E2378A). Half cell potential of steel electrode was obtained by subtracting the EMF from electrode potential of SCE at 30 °C.

Spectroscopic studies

To elucidate the mechanism of interaction of the added compounds on steel rebar immersed in simulated CPS, UV–visible spectroscopic study was performed (Schimadzu UV–visible-1800 spectrophotometer). The spectra of solutions were recorded after 3 days. The oxide film deposited on the steel rebar was carefully scratched with a stainless steel blade, dried and performed FT-IR spectral studies. KBr pellet method was employed to record IR spectra in the range 4000–400 cm^{-1} using Schimadzu IR Affinity-1 model FT-IR spectrophotometer.

Microscopic surface analysis

To investigate the surface morphological changes on the steel rod dipped in simulated concrete pore solution [46, 47], microscopic studies were performed using Leica Stereo Microscope (S8ACO).

Results and discussion

Potentiodynamic polarization studies

Interaction of sodium nitrite with steel rebar

The effect of sodium nitrite concentration on the corrosion of steel rebar in the simulated concrete interstitial solution was investigated using polarization experiments. Data obtained from polarization studies are represented in Table 2. Sodium nitrite solution having concentrations 50–1500 ppm was taken of the study. It is understandable from the polarization data that at very low concentration (50 ppm), sodium nitrite acted as a corrosion antagonist, i.e., the corrosion rate of steel rebar treated with nitrite was greater than that of the rebar immersed in CPS without nitrite (blank). This result warns that one must be very cautious regarding the concentration of the nitrite in concrete when it is employed as an admixture. But as the concentration of nitrite exceed 50 ppm in CPS, the corrosion inhibition efficiency increased. Sodium nitrite showed only 54.84% corrosion inhibition efficiency on steel rebar at a concentration of 1500 ppm in the simulated CPS.

From the Tafel plots (Fig. 1a), it is evident that at lower concentrations of nitrite, the cathodic slopes of polarization curves considerably changed when compared to that of blank steel rebar. But a drastic change in the anodic slopes of Tafel plots observed as the concentration increased. Thus, it can be concluded that at appreciable

Table 2 Potentiodynamic polarization data of steel rebar immersed in contaminated concrete pore solution in the presence and absence of various compounds at 30 °C

System	I_{corr} (μA/cm^2)	b_a (mV/dec^1)	$-b_c$ (mV/dec^1)	$-E_{corr}$ (mV)	η_{pol}%
Blank	45.6	136	222	777.7	–
$NaNO_2$ 50 ppm	52.79	156	192	752.5	− 15.76
$NaNO_2$100 ppm	29.26	155	106	735.2	35.83
$NaNO_2$ 150 ppm	33.09	182	74	751.6	27.56
$NaNO_2$ 200 ppm	36.20	215	83	727.8	20.61
$NaNO_2$ 1500 ppm	20.59	407	176	472.7	54.84
TSC 50 ppm	34.24	142	97	746.1	24.91
TSC 100 ppm	20.01	156	112	742.9	56.11
TSC 150 ppm	15.50	146	81	746.9	66.01
TSC 200 ppm	22.17	177	82	756.2	51.38
TSC 500 ppm	52.92	247	137	723.8	− 16.05
TSC 1100 ppm	53.91	173	284	837.5	− 18.22
TSC 1500 ppm	170.20	254	451	889.1	− 272.0
ZnAc 50 ppm	20.09	167	71	714.9	55.94
ZnAc 100 ppm	22.14	164	78	700.4	51.44
ZnAc 50 ppm + TSC 50 ppm	39.13	160	145	709.0	14.18
ZnAc 50 ppm + TSC 100 ppm	9.021	105	63	789.9	80.23
ZnAc 50 ppm + TSC 150 ppm	10.27	101	95	782.8	77.47
ZnAc 50 ppm + TSC 200 ppm	11.99	104	87	774.8	73.70

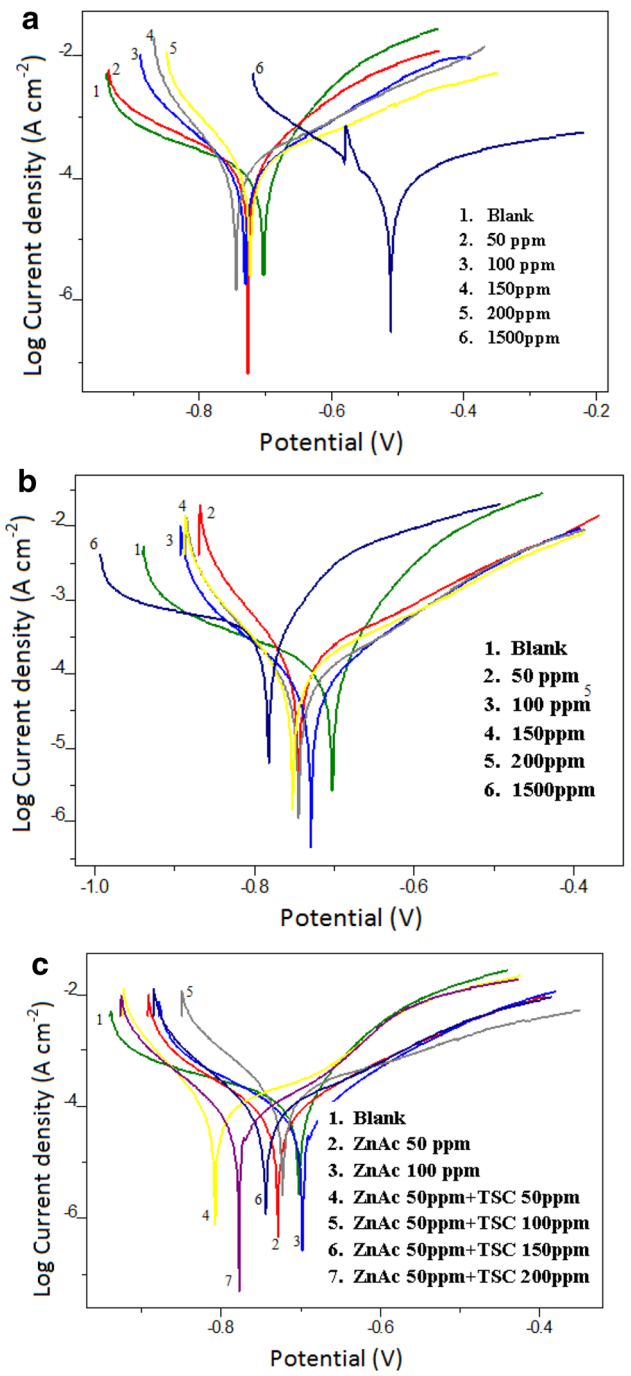

Fig. 1 Tafel curves of steel rebar in contaminated concrete pore solution containing **a** sodium nitrite, **b** TSC and **c** ZnAc and ZnAc + TSC at different concentrations

concentrations, nitrites mainly affect the anodic process of corrosion. It has been established by the earlier researchers that sodium nitrite, an anodic inhibitor, modifies the oxide film on the steel rebar to be more protective than the film that naturally forms in concrete. The inhibitive action of $NaNO_2$ is due to reaction of nitrite ions with Fe^{2+} ions as shown in the following equation [48]:

$$2Fe^{2+} + 2OH^- + 2NO_2^- \rightarrow 2NO \uparrow + Fe_2O_3 + H_2O.$$

Sodium nitrite competes with the chloride ions for ferrous ions produced in concrete and incorporates them into a passive layer on the steel surface, and hence preventing further corrosion.

Interaction of trisodium citrate with steel rebar

Polarization experiments were conducted on steel rebar after an immersion period of 3 days in concrete pore solution containing TSC and 3.5% NaCl (Fig. 1b).

The corrosion protection capacity of TSC on steel rebar was~ 25% at 50 ppm concentration (Table 2). The inhibition efficiency (η_{pol}%) increased with the concentration and a maximum of 66% was reached at 150 ppm of TSC. After this concentration, η_{pol}% started to decrease. At a concentration of 1500 ppm, TSC showed corrosion antagonistic behaviour on steel rebar in CPS. This change of the behaviour of TSC on the steel rebar can be illustrated with the help of two competitive reactions. Citrate ions have a substantial capacity to adsorb on the steel surface from CPS, and hence at lower concentrations they can decrease the rate of corrosion. Simultaneously, citrate ions have a strong tendency to make coordinate bonds with Fe^{2+} ions. The strong complexation between Fe(II) with citrate ions has been well established by Krishnamurthy and Huang [49]. In other words, tendency of TSC to adsorb on steel surface leads to the corrosion inhibition behaviour of the molecule and the affinity of TSC towards ferrous ions favours corrosion antagonistic behaviour. As the concentration of TSC increases, the second process will predominate in the solution over first. This causes to dissolve more and more Fe atoms from the rebar surface to the solution. The mechanism of the interaction of citrate ions on steel rebar surface in CPS can be represented as shown in Fig. 2a. Some of the TSC molecules adsorb on steel surface through oxygen atoms. The species present in the bulk of the solution is Fe(II)–citrate complex. From the figure it can be realized that enhanced dissolution of Fe takes place due to the strong coordinating tendency of citrate ion with ferrous ions.

The behaviour of sodium citrate on steel rebar in concrete pore solution was further verified by electronic spectroscopy. Two significant peaks appeared in the electronic spectrum of TSC in the simulated concrete pore solution at 340 and 217 nm can be explained due to $n \rightarrow \pi^*$ and $\pi \rightarrow \pi^*$ electronic transitions, respectively. CPS contains TSC (1500 ppm) when treated with steel rebar for 3 days, showed three peaks in addition to the above mentioned peaks in UV–visible spectrum. Additional peaks displayed at 682,

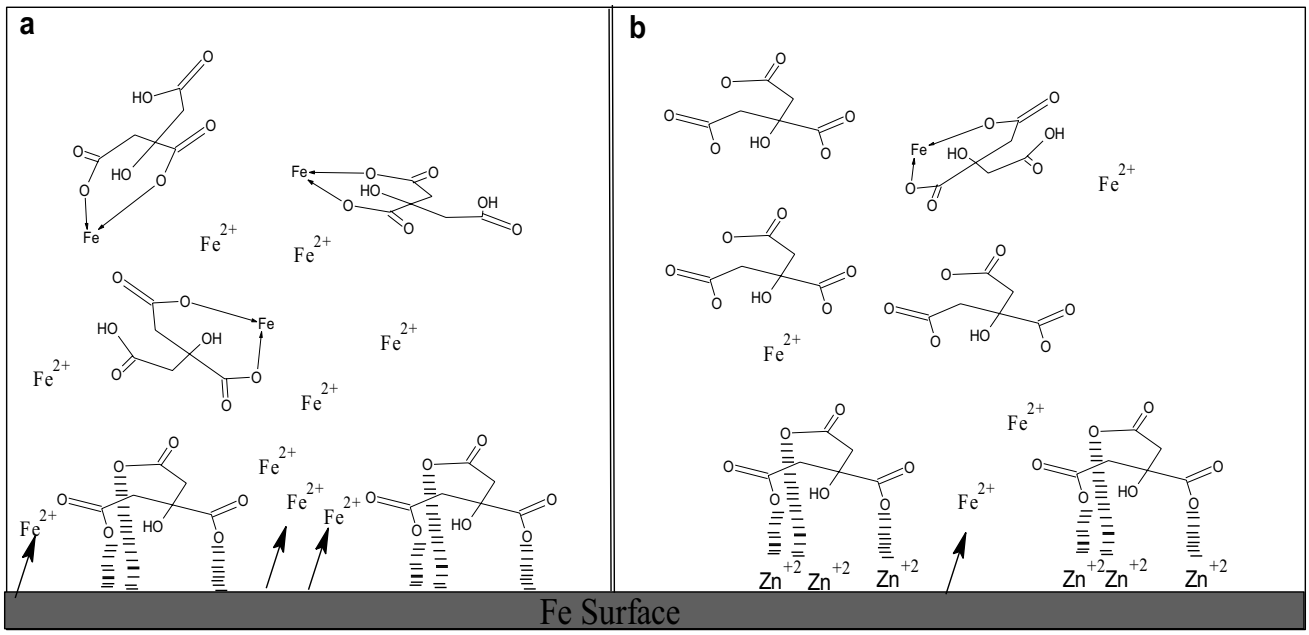

Fig. 2 Interaction of citrate ions on steel surface in simulated concrete pore solution **a** in the absence of zinc acetate and **b** in the presence of zinc acetate

757 and 788 nm can be assigned to the electronic transitions of Fe(II)–citrate complex. Furthermore, it is noticed that the colour of the concrete pore solution containing TSC (1500 ppm) gradually changed into pale green when it was treated with steel rebar. This colour was persisted for ~ 10 days. This indicates the stability of Fe(II)–citrate complex in the alkaline CPS. All other concrete pore test solutions (including nitrite added CPS) were changed into brown colour during 2–3 days. This implies that the Fe(II) ions produced due to corrosion is converting to Fe(III) ions quickly. Hence it can be concluded that the reluctance of Fe(II) to convert into Fe(III) in CPS containing NaCl and TSC is definitely due to the strong complex formation between Fe(II) and citrate ions.

To improve the corrosion inhibition efficiency of TSC on steel rebar, zinc acetate (ZnAc) was added to the concrete pore solution. Table 2 describes the corrosion inhibition efficacy of TSC–ZnAc system and the potentiodynamic polarization parameters of steel rebar. Tafel plots are depicted in Fig. 1c. Data show that η_{pol}% of TSC enhanced appreciably in the presence of zinc acetate. Highest value of η_{pol}% (80.23%) was shown by TSC at 100 ppm in the presence of 50 ppm ZnAc, while it was only 56.11% in the absence of ZnAc. Thus, a drastic depletion in the rate of corrosion of steel rebar was noticed in the presence of TSC–ZnAc mixture in concrete pore solution. This is definitely due to the involvement of zinc ions which favours the strong adsorption of citrate ions on the steel rebar surface [50, 51]. TSC alone did not satisfactorily obey any adsorption isotherm on steel surface. But on the addition of ZnAc, it followed Langmuir adsorption isotherm for a concentration range of 100–200 ppm (Fig. 3).

It can be assumed that affinity of Fe(II) ions to coordinate with citrate ions is minimized considerably in the presence of zinc acetate. This can be easily visualized with the help of Fig. 2b. Zinc ions attach on the steel surface first followed by the adsorption of citrate ions through zinc ions. But as the concentration of TSC increased, the corrosion inhibition efficiency began to decrease slowly. This can be illustrated

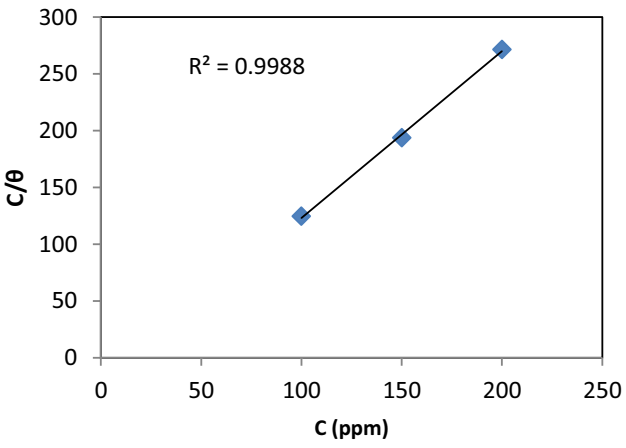

Fig. 3 Langmuir adsorption isotherm for TSC–ZnAc system on steel surface in CPS contaminated with NaCl (TSC 100–200 ppm and ZnAc 50 ppm)

by the same mechanism proposed for of Fe–citrate interaction without ZnAc.

On examination of the polarization data, it is understand that the citrate ion mainly acts on cathodic sites of corrosion. The cathodic slopes of polarization curves of steel rebar in TSC solution were considerably changed than that of blank experiment. Similar trend was observed for the polarization curves of steel rebar in TSC–ZnAc solution (Fig. 1c). The steel rebar treated with concrete pore solution containing 100 ppm of citrate and 50 ppm of zinc acetate displayed least value for cathodic slope in Tafel plot, suggesting that this particular combination has a great influence on the cathodic process of corrosion than any other combination. In alkaline medium, the main half cell reactions responsible for the corrosion are the oxidation of Fe into Fe^{2+} (anodic) and reduction of O_2 into OH^- (cathodic). Citrates and citric acid are well known for its anti-oxidant property [52, 53]. The anti-oxidant property of citrate ion arises due to the scavenging of oxygen molecules. Since citrate ions mainly affect the cathodic sites of corrosion, it can be robustly believed that the oxygen molecules available for the reduction process are considerably reduced in the presence of citrate ions. Thus, it can be concluded that the ability of TSC and TSC–ZnAc systems to decrease the rate of corrosion of steel rebar in concrete pore solution is due to the combined action of adsorption and scavenging of oxygen molecules.

Comparison of η_{pol}% of various systems on steel rebar in CPS contaminated with 3.5% NaCl at 30 °C is shown in Fig. 4.

Half cell potential measurements

Measurement of half cell potential of steel rebar gave a rough idea about the probability of corrosion. It has been generally accepted by the scientists that more negative the half cell potential, greater will be the possibility of corrosion.

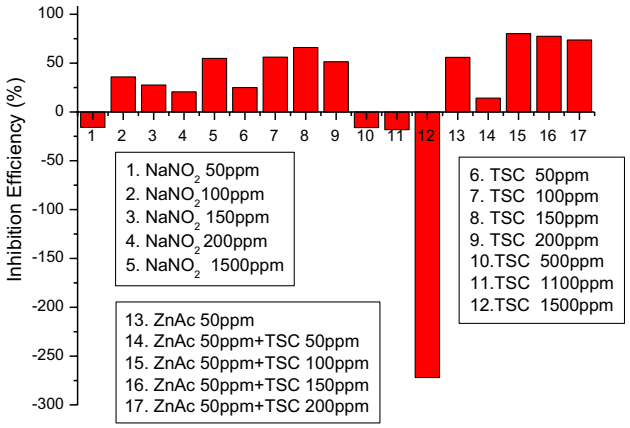

Fig. 4 Comparison of η_{pol}% of various systems on steel rebar in simulated concrete pore solution contaminated with 3.5% NaCl at 30 °C

Half cell potentials of steel rebar immersed in concrete pore solution for a period of 24 h in the presence and absence of various compounds are given in Table 3 and compared with the help of a bar diagram (Fig. 5). According to the data, the steel rebar immersed in concrete pore solution (blank) showed a potential of −460 mV against SCE. This is a clear indication of high corrosion rate of steel rebar. A regular increase of electrode potential (towards cathodic) was noted with the addition of TSC. But as the concentration reached to 200 ppm, electrode potential shifted to more anodic side. At 1500 ppm of TSC concentration, the electrode potential of the steel rebar was −518 mV, indicating that the corrosion rate of steel rebar increased tremendously. Both half cell potential measurements and polarization studies revealed the similar corrosion behaviour of steel rebar in CPS solution. On comparing the potentials of steel rebars in CPS–$NaNO_2$ solution with those rebars treated with CPS–TSC solution, it can be concluded that TSC is acting as a better corrosion inhibiting agent than nitrite at lower concentrations. The steel rebar treated with concrete pore solution containing 100 ppm TSC and 50 ppm ZnAc displayed very low

Table 3 Half cell potential (mV) measured on steel rebar immersed in contaminated CPS-containing $NaNO_2$, TSC and TSC–ZnAc systems at 24 h

C (ppm)	$NaNO_2$	TSC	TSC + ZnAc (50 ppm)
0	−460	−460	−460
50	−358	−333	−349
100	−338	−314	−283
150	−328	−307	−304
200	−346	−316	−307
1500	−293	−518	−508

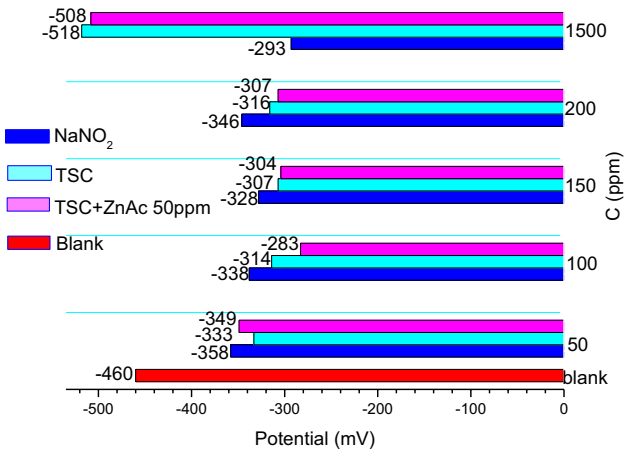

Fig. 5 Comparison of half cell potentials of steel rebar in simulated contaminated concrete pore containing $NaNO_2$, TSC and TSC–ZnAc systems

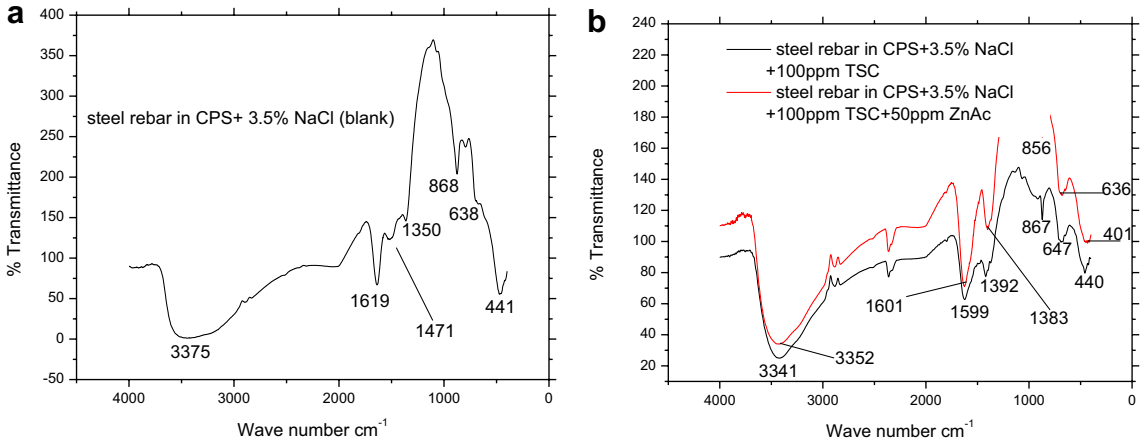

Fig. 6 IR spectrum of oxide film deposited on steel rebar in simulated concrete pore solution **a** contaminated with 3.5% NaCl, **b** containing 3.5% NaCl + 100 ppm TSC and 3.5% NaCl + 100 ppm TSC + 50 ppm ZnAc

anodic potential (− 283 mV), suggesting that this particular combination works well on the steel surface to reduce the corrosion. Similar result was obtained by potentiodynamic polarization studies.

FT-IR analysis

To investigate mechanism of molecular interaction on steel surface in simulated CPS, IR spectral studies were performed. Due to the presence of many species in the simulated concrete pore solution, it is rather difficult to interpret the spectrum of deposited products on steel rebar surface completely. However, on close inspection of the spectra, it is obvious that considerable shift in the frequencies occurred for the samples treated with and without ZnAc. Surface deposition of steel rebar is mainly consists of mixtures of compounds such as hydrated ferric oxide, ferrous and ferric hydroxides, ferrous chloride. In the IR spectrum of products on steel rebar surface (blank), a broad band appeared at 3375 cm^{-1} is due to –OH stretching frequency of $Fe(OH)_2$ or amorphous hydrated ferric oxide (or both) [54]. The broadness of this peak is considerably reduced in the IR spectra of steel samples treated with TSC and TSC–ZnAc. This is due to the interaction of these species with $Fe(OH)_2$. The bending frequency of –OH appeared in the spectrum of blank (at 1619 cm^{-1}) was also shifted to lower frequency side in other two samples. Signals observed at ~ 440 cm^{-1} in the IR spectrum of blank and citrate-treated steel rebar are lowered to 401 cm^{-1} in TSC–ZnAc-treated steel rebar. This can be attributed to the change of lattice vibration of free OH^- ions due to the interaction O–H–Zn–citrate. Peaks displayed at 1392 and 1383 cm^{-1} in the IR spectra of two samples are due to the deformation of $–CH_2$ group present in sodium citrate. A weak peak appeared at 1471 cm^{-1} in the IR spectrum of surface products of blank specimen is due to the existence of ferroxyhite phase associated with the amorphous ferric oxide on the steel surface. Figure 6 represents the IR spectrum of products deposited on steel rebar surface.

Microscopic surface analysis

Visual examination of the micrographs showed that the ferric oxide layer formed on the steel rod immersed in the sample solutions was uneven, brittle, blistered and black in colour, quite different from the bare, where it was dark brown in colour. The removal of oxide film from the immersed steel rebars was easier due to the non-uniform distribution over the surface as compared to the bare where it was tightly adherent. The textures of immersed steel rods in CPS were different from each other and they also differed from the bare sample. The surface morphology of the steel sample treated with concrete pore solution containing TSC 1500 ppm got a unique appearance as its surface do not contains little or no oxide deposit. The complexing nature of citrate ions with Fe^{2+} enhanced the removal of more and more Fe atoms from the surface of rebar into the solution (Fig. 7).

Conclusions

Electrochemical studies of steel rebar in simulated concrete interstitial solution established the corrosion behaviour in the presence of various compounds. At low concentrations, $NaNO_2$ acted as a corrosion accelerator. As the concentration of $NaNO_2$ increased protection efficiency increased. Generally, trisodium citrate exhibited better protection capacity than $NaNO_2$. However, in the presence of TSC–zinc acetate system very appreciable lowering of the corrosion rate was noticed. According to Tafel polarization studies, steel rebar is well protected in concrete pore solution contaminated with

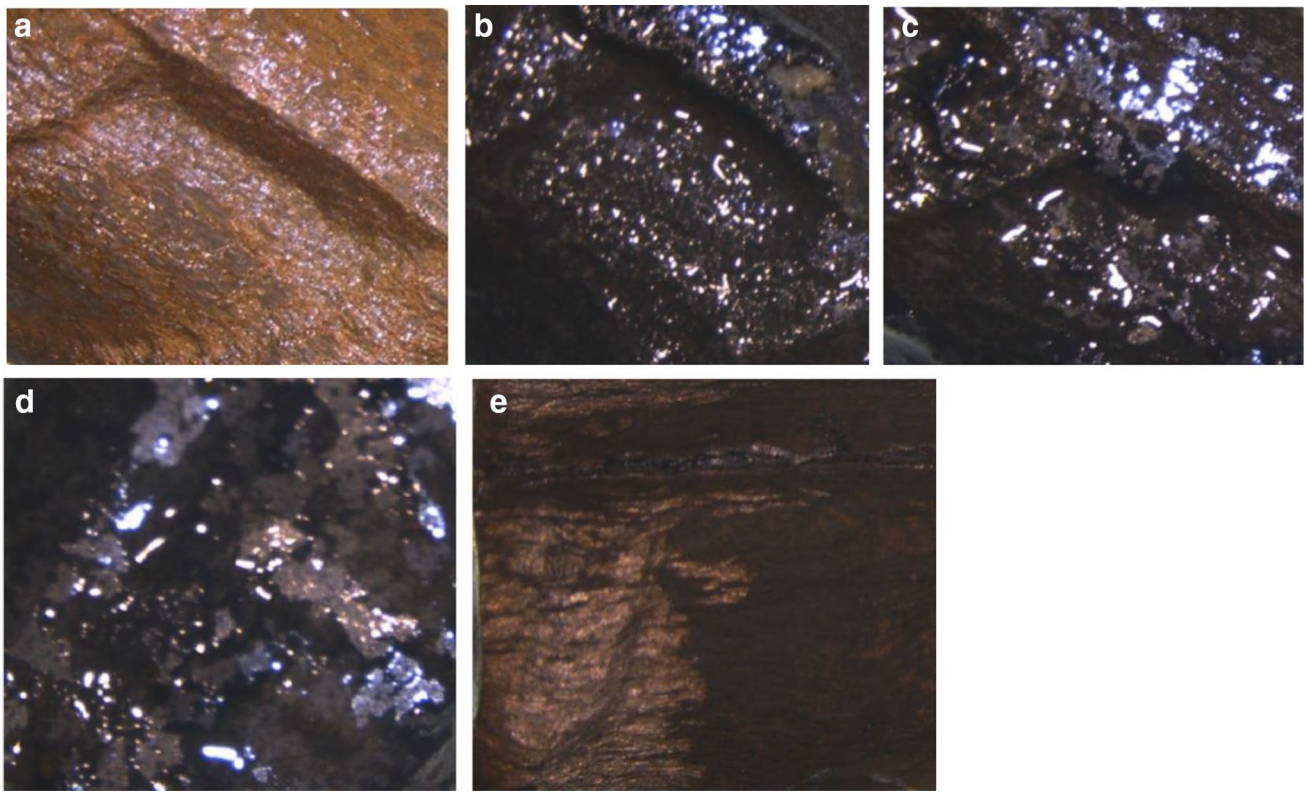

Fig. 7 Optical micrographs of Fe rebar **a** bare surface, **b** immersed in concrete pore solution contaminated with 3.5% NaCl (blank) **c** with NaCl (3.5%) + TSC 100 ppm **d** with NaCl (3.5%) + TSC 100 ppm + ZnAc50 ppm **e** with NaCl (3.5%) + TSC 1500 ppm at 30 °C (samples **b**–**e**, immersed in CPS for 3 days)

3.5% NaCl by TSC 100 ppm–ZnAc 50 ppm system. Half cell potential measurements gave an idea about the probability of corrosion. Mainly, the rate of cathodic process of steel corrosion was suppressed by TSC and TSC–ZnAc systems in concrete pore solution. FT-IR and UV–visible spectral studies and optical microscopic investigations revealed the mechanism of interaction of compounds on steel rebar.

References

1. Moreno M, Morris W, Alvarez MG, Duffó GS (2004) Corrosion of reinforcing steel in simulated concrete pore solutions. Corros Sci 46:2681–2699
2. Abd El Wanees S, Bahgat Radwan A, Alsharif MA, Abd El Haleem SM (2017) Initiation and inhibition of pitting corrosion on reinforcing steel under natural corrosion conditions. Mater Chem Phys 190:79–95
3. Abd El Haleem SM, Abd El Wanees S, Abd El Aal EE, Diab A (2010) Environmental factors affecting the corrosion behavior of reinforcing steel II. Role of some anions in the initiation and inhibition of pitting corrosion of steel in $Ca(OH)_2$ solutions. Corros Sci 52:292–302
4. Abd El Haleem SM, Abd El Wanees S, Abd El Aal EE, Diab A (2010) Environmental factors affecting the corrosion behavior of reinforcing steel IV. Variation in the pitting corrosion current in relation to the concentration of the aggressive and the inhibitive anions. Corros Sci 52:1675–1683
5. Abd El Aal EE, Abd El Wanees S, Diab A, Abd El Haleem SM (2009) Environmental factors affecting the corrosion behavior of reinforcing steel III. Measurement of pitting corrosion currents of steel in $Ca(OH)_2$ solutions under natural corrosion conditions. Corros Sci 51:1611–1618
6. Valcarce MB, Vázquez M (2008) Carbon steel passivity examined in alkaline solutions: the effect of chloride and nitrite ions. Electrochim Acta 53:5007–5015
7. Montemor MF, Simoes AMP, Ferreira MGS (2003) Chloride-induced corrosion on reinforcing steel: from the fundamentals to the monitoring techniques. Cem Concr Compos 25:491–502
8. Ormellese M, Lazzari L, Goidanich S, Fumagalli G, Brenna AA (2009) Study of organic substances as inhibitors for chloride-induced corrosion in concrete. Corros Sci 51:2959–2968
9. Pandiarajan M, Prabhakar P, Rajendran S (2013) Corrosion resistance of mild steel in simulated concrete pore solution. Chem Sci Trans 2(2):605–613

10. Elsener B, Büchler M, Stalder F, Böhni H (2000) Migrating corrosion inhibitor blend for reinforced concrete: part 2—inhibitor as repair strategy. Corrosion 56:727–732
11. Dhouibi L, Triki E, Raharinaivo A (2002) The application of electrochemical impedance spectroscopy to determine the long-term effectiveness of corrosion inhibitors for steel in concrete. Cem Concr Compos 24:35–43
12. Rincón OT, Pérez O, Paredes E, Caldera Y, Urdaneta C, Sandoval I (2002) Long-term performance of ZnO as a rebar corrosion inhibitor. Cem Concr Compos 24:79–87
13. Liang H, Li L, Poor ND, Sagüés AA (2003) Nitrite diffusivity in calcium nitrite-admixed hardened concrete. Cem Concr Res 33:139–146
14. Cigna R, Proverbio E, Rocchini G (1993) A study of reinforcement behaviour in concrete structures using electrochemical techniques. Corros Sci 35:1579–1584
15. Oranowska H, Szklarska-Smialowska Z (1981) An electrochemical and ellipsometric investigation of surface films grown on steel in saturated calcium hydroxide solutions with or without chloride ions. Corros Sci 21:735–747
16. Joiret S, Keddam M, Nóvoa XR, Pérezb MC, Rangelc C, Takenouti H (2002) Use of EIS, ring-disk electrode, EQCM and Raman spectroscopy to study the film of oxides formed on steel in 1 M NaOH. Cem Concr Compos 24:7–15
17. Andrade C, Keddam M, Nóvoa XR, Pérez MC, Rangel CM, Takenouti H (2001) Electrochemical behaviour of steel rebars in concrete: influence of environmental factors and cement chemistry. Electrochim Acta 46:3905–3912
18. Kitowski CJ, Wheat HG (1997) Effect of chlorides on reinforcing steel exposed to simulated concrete solutions. Corrosion 53:216–226
19. Ann KY, Song HW (2007) Chloride threshold level for corrosion of steel in concrete. Corros Sci 49:4113–4133
20. Trépanier S, Hope B, Hansson C (2001) Corrosion inhibitors in concrete. Cem Concr Res 31:713–718
21. Jiang L, Huang G, Xu J, Zhu Y, Mo L (2012) Influence of chloride salt type on threshold level of reinforcement corrosion in simulated concrete pore solutions. Constr Build Mater 30:516–521
22. Morris W, Vázquez MA (2002) Migrating corrosion inhibitor evaluated in concrete containing various contents of admixed chlorides. Cem Concr Res 32:259–267
23. Rosenberg A (2000) Discussion: migrating corrosion inhibitor blend for reinforcing concrete: part 1—prevention of corrosion. Corrosion 56:986–987
24. Monticelli C, Frignani A, Trabanelli GA (2000) Study on corrosion inhibitors for concrete application. Cem Concr Res 30:635–642
25. Al-Amoudi OSB, Maslehuddin M, Lashari A, Almusallam AA (2003) Effectiveness of corrosion inhibitors in contaminated concrete. Cem Concr Compos 25:439–449
26. Elsener B, Büchler M, Stalder F, Böhni H (2000) Migrating corrosion inhibitor blend for reinforced concrete: part 2—inhibitor as repair strategy. Corrosion 56(7):727–732
27. Andrade C, Alonso C, Acha M, Malric B (1992) Preliminary testing of Na_2PO_3F as a curative corrosion inhibitor for steel reinforcements in concrete. Cem Concr Res 22:869–881
28. Berke NS, Hicks MC (2004) Predicting long-term durability of steel reinforced concrete with calcium nitrite corrosion inhibitor. Cem Concr Compos 26:191–198
29. Wellea A, Liao JD, Kaiser K, Grunze M, Mäder U (1997) Blank *N* interactions of *N*, *N*-dimethylaminoethanol with steel surfaces in alkaline and chlorine containing solutions. Appl Surf Sci 119:185–198
30. Reou S, Ann KY (2008) The electrochemical assessment of corrosion inhibition effect of calcium nitrite in blended concretes. Mater Chem Phys 109:526–533
31. Ryu H-S, Singh JK, Lee H-S, Ismail MA, Park W-J (2017) Effect of $LiNO_2$ inhibitor on corrosion characteristics of steel rebar in saturated $Ca(OH)_2$ solution containing NaCl: an electrochemical study. Constr Build Mater 133:387–396
32. Ryu H-S, Singh JK, Lee H-S, Park W-J (2017) An electrochemical study to evaluate the effect of calcium nitrite inhibitor to mitigate the corrosion of reinforcement in sodium chloride contaminated $Ca(OH)_2$ solution. Adv Mater Sci Eng 2017:6265184. https://doi.org/10.1155/2017/6265184
33. Ngala V, Page C, Page M (2002) Corrosion inhibitor systems for remedial treatment of reinforced concrete. Part 1: calcium nitrite. Corros Sci 44:2073–2087
34. Ryu H-S, Singh JK, Yang HM, Lee H-S, Ismail MA (2016) Evaluation of corrosion resistance properties of *N*, *N*'-dimethyl ethanolamine corrosion inhibitor in saturated $Ca(OH)_2$ solution with different concentrations of chloride ions by electrochemical experiments. Constr Build Mater 114:223–231
35. Hassoune M, Bezzar A, Sail L, Ghomari F (2017) Corrosion inhibition of carbon steel by *N*, *N*′-dimethylaminoethanol in simulated concrete pore solution contaminated with NaCl. J Adhes Sci Technol 32:68–90
36. Elsener B, Büchler M, Stalder F, Böhni H (1999) Migrating corrosion inhibitor blend for reinforced concrete: part 1—prevention of corrosion. Corrosion 55:1155–1163
37. Berke NS, Dallaire MP, Hicks MC, Hoopes RJ (1993) Corrosion of steel in cracked concrete. Corrosion 49:934–943
38. Saremi M, Mahallati E (2002) A study on chloride-induced depassivation of mild steel in simulated concrete pore solution. Cem Concr Res 32:1915–1921
39. Tang YM, Miao YF, Zuo Y, Zhang GD, Wang CL (2012) Corrosion behavior of steel in simulated concrete pore solutions treated with calcium silicate hydrates. Constr Build Mater 30:252–256
40. Hansson C, Mammoliti L, Hope B (1998) Corrosion inhibitors in concrete part I: the principles. Cem Concr Res 28:1775–1781
41. Li L, Sagüés AA (2002) Chloride corrosion threshold of reinforcing steel in alkaline solutions—cyclic polarization behavior. Corrosion 58:305–316
42. García Calvo JL, Sánchez Moreno M, Alonso Alonso MC, Hidalgo López A, García Olmo J (2013) Study of the microstructure evolution of low-ph cements based on ordinary portland cement (opc) by mid- and near-infrared spectroscopy, and their influence on corrosion of steel reinforcement. Materials 6(6):2508–2521. https://doi.org/10.3390/ma6062508
43. Stern MA (1958) Method for determining corrosion rates from linear polarization data. Corrosion 14:60–64
44. Flitt HJ, Schweinsberg DP (2005) Evaluation of corrosion rate from polarisation curves not exhibiting a Tafel region. Corros Sci 47:3034–3052
45. Elsener B (2005) Corrosion rate of steel in concrete—measurements beyond the Tafel law. Corros Sci 47:3019–3033
46. Olefjord I, Wegrelius L (1990) Surface analysis of passive state. Corros Sci 31:89–98
47. Veleva L, Alpuche-Aviles MA, Graves-Brook MK, Wipf DO (2002) Comparative cyclic voltammetry and surface analysis of passive films grown on stainless steel 316 in concrete pore model solutions. J Electroanal Chem 537:85–93
48. Maan H, Shatha AS, Adeeb H, Inas MA (2012) Utilizing of sodium nitrite as inhibitor for protection of carbon steel in salt solution. Int J Electrochem Sci 7:6941–6950
49. Krishnamurti SR, Huang PM (1991) Influence of citrate on the kinetics of Fe(II) oxidation and the formation of steel oxyhydroxides. Clays Clay Miner 39(1):28–34

50. Naderi R, Mahdavian M, Attar MM (2002) Electrochemical behavior of organic and inorganic complexes of Zn(II) as corrosion inhibitors for mild steel: solution phase study. Electrochim Acta 54:6892–6895
51. Mahdavian M, Naderi R (2011) Corrosion inhibition of mild steel in sodium chloride solution by some zinc complexes. Corros Sci 53:1194–1200
52. Ciriminna R, Meneguzzo F, Delisi R, Pagliaro M (2017) Citric acid: emerging applications of key biotechnology industrial product. Chem Cent J. https://doi.org/10.1186/s13065-017-0251-y
53. Abdel-Salam OME, Youness ER, Mohammed NA, Morsy SMY, Omara EA, Sleem AA (2014) Citric acid effects on brain and liver oxidative stress in lipopolysaccharide-treated mice. J Med Food 17:588–598
54. Fathima PM, Umapathy S, Dhanalakshmi V, Anbarasam R (2010) Synthesis and characterizations of nanosized iron(II) hydroxide and iron(II)hydroxide/poly(vinylalcohol) nanocomposite. J Appl Polym Sci 118:1728–1737